J Mol Model (2011) 17:2285–2296
DOI 10.1007/s00894-011-1038-z

ORIGINAL PAPER

Theoretical evaluation of isotopic fractionation factors in oxidation reactions of benzene, phenol and chlorophenols

Paweł Adamczyk · Piotr Paneth

Received: 15 September 2010 / Accepted: 11 March 2011 / Published online: 27 April 2011

Abstract We have studied theoretically the rate determining steps of reactions of benzene with permanganate, perchlorate, ozone and dioxygen in the gas phase and aqueous solution as well as phenol and dichlorophenol in protonated and unprotonated forms in aqueous solution. Kinetic isotope effects were then calculated for all carbon atoms and based on their values isotopic fractionation factors corresponding to compound specific isotopic analysis have been evaluated. The influence of the oxidant, substituents, environment and protonation on the isotopic fractionation factors has been analyzed.

Keywords Aromatic pollutants · CSIA · DFT · Isotopic fractionation · Permanganate

Introduction

Aromatic compounds constitute a group of persistent, health-threatening [1–4] pollutants [5] that are found in air, soil, sediments, surface water and groundwater [6–9]. Benzene, a model aromatic compound, phenol, and its chlorinated derivatives are commonly found in the environment due to industrial emissions, discharge and wastes, oil and gasoline and emission of their incomplete combustion, or tobacco smoke [1, 3–6, 10]. Degradation of these pollutants can be performed in several ways – biological, thermal and chemical. As biological methods require long degradation time [11], especially phenols (which in high concentration can even make this treatment impractical [12]), and applicability of thermal methodology is limited by emission of hazardous compounds [13], in situ chemical oxidation (ISCO) seems to be a good alternative. Chemical oxidation of groundwater contaminants is usually carried out by direct injections of a chemical oxidant such as permanganate, perchlorate, ozone or even oxygen, alone or in combinations [12–15]. Permanganate is one of the most common oxidizing agents with a unique affinity towards organic compounds with carbon-carbon double bond and hydroxyl or aldehyde groups [15]. Chemical oxidation with permanganate is a very popular method in degradation of organic contaminants due to its rapidity, effectiveness, wide pH range and relatively low cost. Ozonation is also popular in degradation of organic compounds. Other oxidation treatments are based on production of a hydroxyl radical that is a stronger oxidant then many commonly used chemical reagents [16]. Application of these methods to water contaminants seems to be very attractive but they are still under development and have some limitations, such as narrow pH range and high cost [17, 24].

The mechanism of reactions of aliphatic compounds with ozone is similar to that of oxidation by permanganate [18], however, ozonation of aromatic compounds is not fully understood [19–21]. It is energetically more demanding and the barrier increases with the number of substituents of the aromatic ring [15, 22]. Reactions with perchlorate and dioxygen also remain not fully explored. Recently, compound specific isotopic analysis (CSIA) became a useful tool in investigating remediation processes [23–26]. This isotope ratio analysis can yield information about the mechanism of a reaction and can be used for studying behavior and fate of pollutants [26–28]. It is

P. Adamczyk · P. Paneth (✉)
Institute of Applied Radiation Chemistry, Faculty of Chemistry,
Technical University of Lodz,
Zeromskiego 116,
90–924 Lodz, Poland
e-mail: paneth@p.lodz.pl

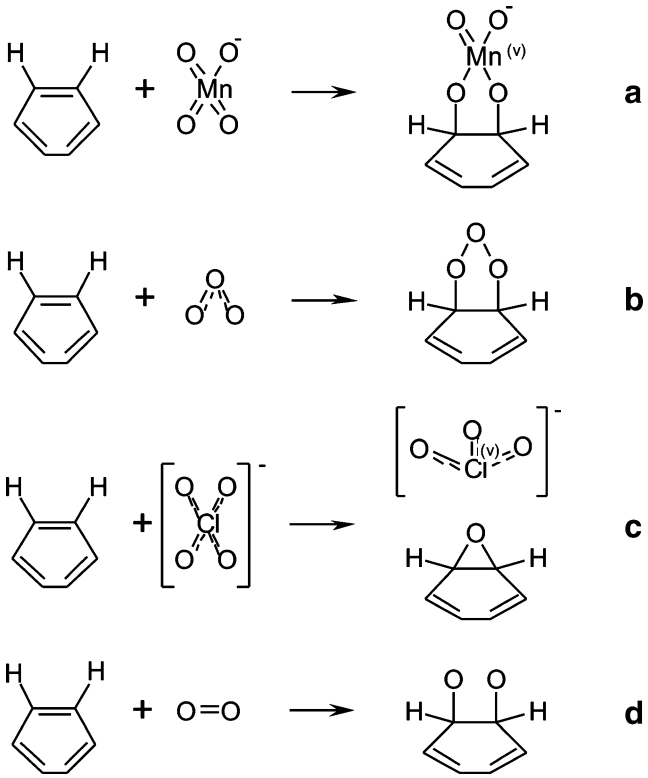

Fig. 1 Modeled benzene oxidation by: (**a**) permanganate, (**b**) ozone, (**c**) perchlorate, (**d**) dioxygen

based on monitoring changes of the isotopic composition of reactants or products that result from the differences in the rate constants of molecules containing different isotopes in the reactive positions. Since CSIA averages

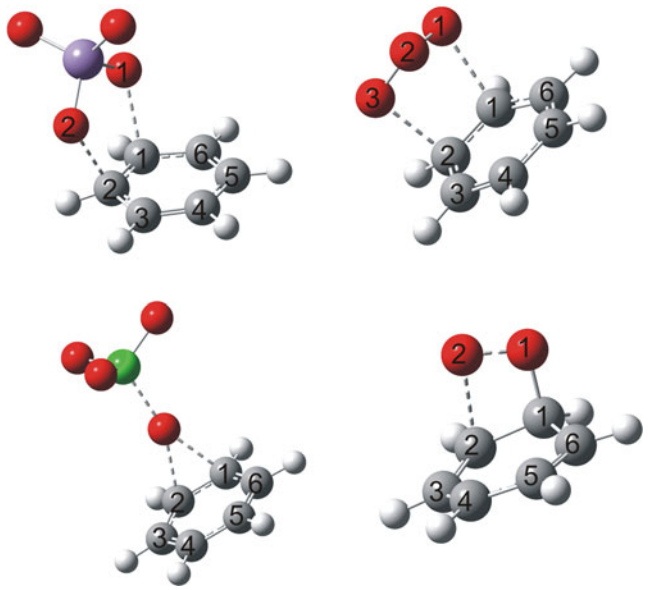

Fig. 2 Optimized structures of transition states of benzene oxidation by (from upper, left) permanganate, ozone, perchlorate and dioxygen

Table 1 Activation Gibbs free energies and exothermicity of benzene oxidation

Oxidant	Gas phase		Liquid phase	
	$\Delta G^{\neq}$ [kcal/mol]	ΔG_R [kcal/mol]	$\Delta G^{\neq}$ [kcal/mol]	ΔG_R [kcal/mol]
MnO_4^-	28.9	−40.7	21.2	−45.6
O_3	15.2	−25.2	13.6	−28.0
ClO_4^-	57.4	−7.8	49.4	−10.4
O_2	24.9	−5.1	41.7	−8.5

isotopic fractionation of all atoms of a given element in order to draw mechanistic conclusions it is important to learn the isotopic fractionations at all sites for the model compounds. To this effect we have carried out theoretical studies of abiotic degradation pathways of benzene, phenol and chlorophenols. On the example of benzene we have compared oxidation by different oxidants; permanganate, ozone, perchlorate, and dioxygen. The influence of the pH and polarity has been evaluated for these reactions by performing calculations in the gas phase and in a model of the aqueous solution. Then we have concentrated on oxidative degradations of phenol and its dichloroderivative with permanganate in aqueous solution. In these studies we have evaluated the influence of substituents and the protonation state.

Methodology

All calculations were performed using the Gaussian package (versions G03 rev. E.01 [27], and G09 rev. A.02 [28]) at the M05-2X/6-31 G+(d,p) [29–35] level of theory. For aqueous solution calculations IEFPCM solvent model [36] with UFF [37] atom radii was used. This theory level has been shown to yield good results at reasonable cost [38] for dehalogenation of trichloroethene. All oxidants were modeled in singlet state, in the case of ozone, an unrestricted open shell method [39] was used. All structures have been optimized with default convergence criteria and characterized by the vibrational analysis. Transition states were found using the Berny algorithm [40, 41], the reaction paths were investigated with IRC [42] procedure and the end points were optimized to reactants or products. The vibrational analysis was carried out to confirm that the obtained geometries correspond to stationary points on the potential energy surfaces (transition states, reactants, or products) and to evaluate reaction, Gibbs free energies and to calculate kinetic isotope effects (KIEs) using the ISOEFF [43] package. ^{13}C-KIEs of each position were calculated according to the Bigeleisen

Table 2 Selected geometric parameters[a] of modeled oxidation processes (R – reactants, TS – transition states, P – products)

	Gas phase			Liquid phase		
	R	TS	P	R	TS	P
MnO_4^-						
d_{C1-C2}	1.395	1.421	1.531	1.395	1.419	1.558
d_{C1-O1}	3.367	2.026	1.406	4.017	2.086	1.427
d_{C2-O2}	3.194	2.026	1.411	3.989	2.086	1.427
d_{O1-Mn}	1.577	1.625	1.826	1.572	1.618	1.792
d_{O2-Mn}	1.577	1.625	1.823	1.572	1.618	1.792
$\alpha_{O1-C1-C2}$	121.3	105.4	107.5	97.4	104.8	109.6
$\alpha_{C1-C2-O2}$	79.1	105.4	108.0	99.3	104.8	109.6
$\alpha_{C2-O2-Mn}$	130.3	114.5	111.4	116.3	115.0	115.9
$\alpha_{O2-Mn-O1}$	108.7	100.3	88.5	109.5	100.4	89.0
$\alpha_{Mn-O1-C1}$	100.1	114.5	112.0	115.9	115.0	115.9
O_3						
d_{C1-C2}	1.395	1.435	1.557	1.396	1.435	1.557
d_{C1-O1}	3.037	2.078	1.449	3.073	2.117	1.449
d_{C2-O3}	3.159	2.078	1.449	3.326	2.117	1.449
d_{O1-O2}	1.237	1.283	1.414	1.236	1.284	1.414
d_{O3-O2}	1.241	1.283	1.414	1.240	1.284	1.414
$\alpha_{O1-C1-C2}$	92.6	99.3	102.6	89.0	99.2	102.6
$\alpha_{C1-C2-O3}$	97.7	99.3	102.6	102.5	99.2	102.6
$\alpha_{C2-O3-O2}$	80.7	98.3	102.3	76.7	98.1	102.3
$\alpha_{O3-O2-O1}$	117.7	110.5	101.4	117.6	110.6	101.4
$\alpha_{O2-O1-C1}$	94.3	98.3	102.3	98.8	98.1	102.3
ClO_4^-						
d_{C1-C2}	1.395	1.428	1.514	1.396	1.411	1.508
d_{C1-O}	3.436	2.009	1.437	3.987	1.971	1.435
d_{C2-O}	4.198	1.722	1.425	3.955	1.968	1.435
d_{O-Cl}	1.486	1.968	5.099	1.481	1.965	3.207
$\alpha_{O-C1-C2}$	113.8	57.2	57.7	78.6	68.9	58.3
$\alpha_{C1-C2-O}$	48.5	78.7	58.5	81.1	69.1	58.3
$\alpha_{C1-O-C2}$	17.7	44.2	63.9	20.2	42.0	63.4
$\alpha_{C1-O-Cl}$	102.4	170.4	35.2	140.8	159.6	143.8
$\alpha_{C2-O-Cl}$	84.7	141.2	91.7	161.1	158.4	151.8
O_2						
d_{C1-C2}	1.391	1.496	1.528	1.391	1.513	1.530
d_{C1-O1}	2.989	1.447	1.454	2.974	1.447	1.463
d_{C2-O2}	3.007	2.509	1.459	2.965	2.235	1.469
d_{O1-O2}	1.202	1.411	1.464	1.204	1.364	1.463
$\alpha_{O1-C1-C2}$	88.2	108.6	88.1	88.2	103.8	88.1
$\alpha_{C1-C2-O2}$	88.2	65.1	87.8	88.2	69.4	87.9
$\alpha_{C2-O2-O1}$	91.0	68.7	90.4	92.2	76.4	90.5
$\alpha_{O2-O1-C1}$	92.6	108.4	90.6	91.4	104.0	90.7

[a] d – distances in Å, α – angles in °

Table 3 Calculated carbon kinetic isotope effects and CSIA fractionation factors on benzene reactions with studied oxidants

Position	Gas chase				Liquid phase			
	MnO_4^-	O_3	ClO_4^-	O_2	MnO_4^-	O_3	ClO_4^-	O_2
C_1	1.0215	1.0219	1.0127	1.0046	1.0204	1.0211	1.0117	1.0005
C_2	1.0219	1.0214	1.0190	1.0155	1.0207	1.0209	1.0118	1.0251
C_3	1.0007	1.0002	1.0020	1.0051	1.0004	1.0002	1.0008	1.0076
C_4	1.0012	1.0014	1.0012	1.0072	1.0019	1.0011	1.0012	1.0068
C_5	1.0016	1.0008	1.0028	1.0061	1.0023	1.0009	1.0015	1.0040
C_6	1.0007	1.0003	1.0010	1.0049	1.0003	1.0006	1.0010	1.0040
ε_{CSIA} [‰]	−7.88	−7.57	−6.42	−7.21	−7.62	−7.36	−4.65	−8.33

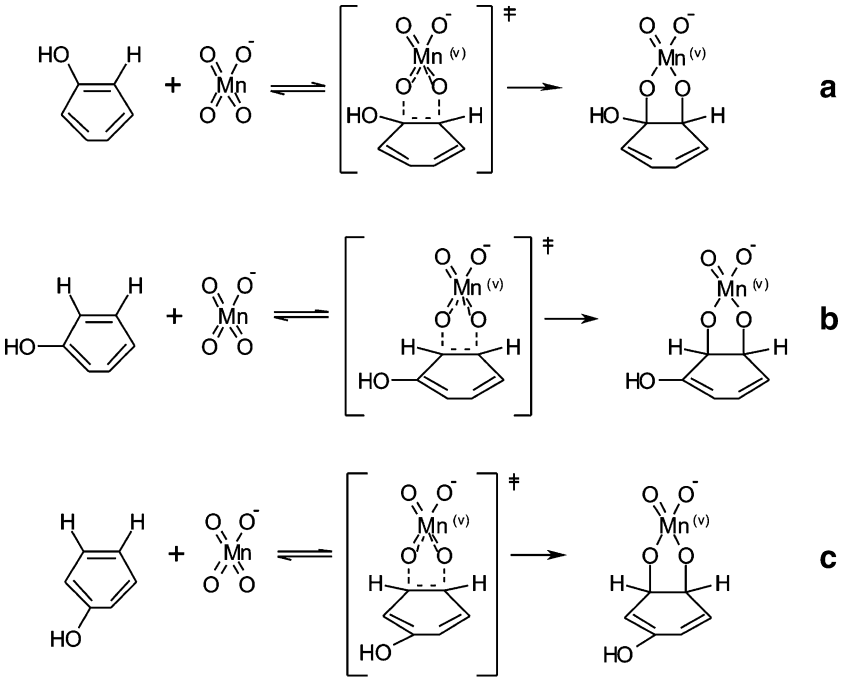

Fig. 3 Modeled reactions of permanganate with protonated form of phenol, Attack at the position (**a**) C_1-C_2, (**b**) C_2-C_3, (**c**) C_3-C_4

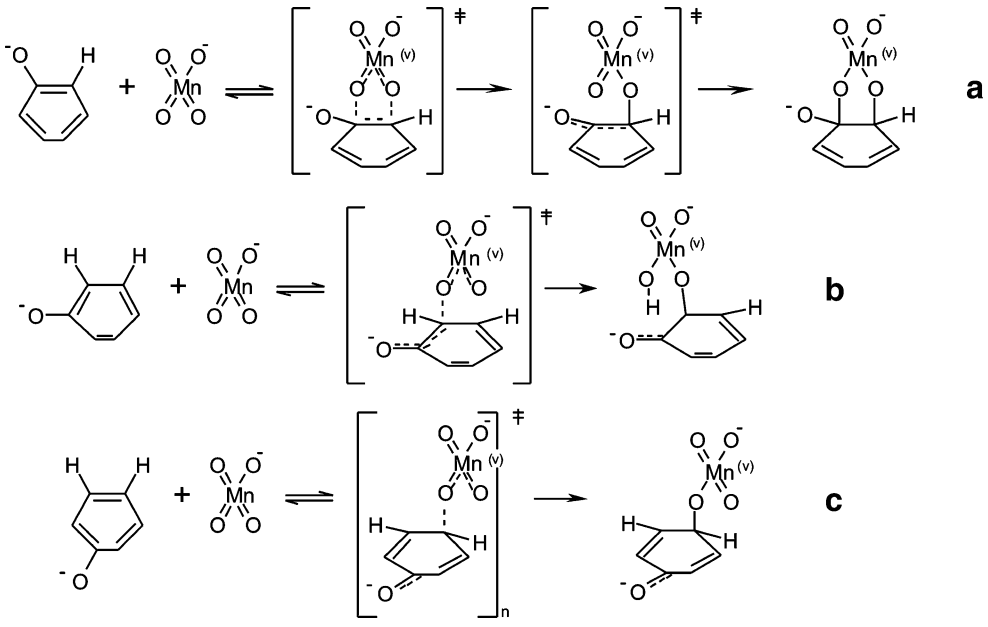

Fig. 4 Modeled reactions of permanganate with deprotonated form of phenol, Attack at the position (**a**) C_1-C_2, (**b**) C_2-C_3, (**c**) C_3-C_4

Table 4 Activation Gibbs free energies and exothermicity of investigated reactions of protonated and deprotonated form of phenol with permanganate ion

	Protonated form		Deprotonated form	
	$\Delta G^{\neq}$ [kcal/mol]	ΔG_R [kcal/mol]	$\Delta G^{\neq}$ [kcal/mol]	ΔG_R [kcal/mol]
C_1-C_2	27.2	−49.0	15.9	−41.1
C_2-C_3	27.1	−45.4	14.7	−76.9
C_3-C_4	22.9	−46.6	16.1	−28.7

equation [44] and converted to carbon isotopic fractionation factors, ε [‰], according to Eq. 1. CSIA fractionation factors were then calculated as the average values of the obtained isotopic fractionation factors of all six individual positions. This approach corresponds to an approximation that only singly labeled molecules are considered [45].

$$\varepsilon = (1/\mathrm{KIE} - 1) \cdot 1000 \quad (1)$$

Results and discussion

Benzene

In the case of benzene we have considered the reactions with four different oxidants: permanganate, ozone, perchlorate, and dioxygen in the gas phase and in the aqueous solution. The rate determining step of these reactions, illustrated schematically in Fig. 1, is the addition of the oxidant to the unsaturated bond of the ring. Thus isotopic fractionation of this step may be compared directly with the experimental data. Figure 2 shows optimized structures of the corresponding transition states together with atom numbering used in the following discussion. No bridging structures of the transition states, corresponding to the attack at carbon atoms positions 1 and 3 or 1 and 4 were identified; such initial structures converged to those presented in Fig. 2.

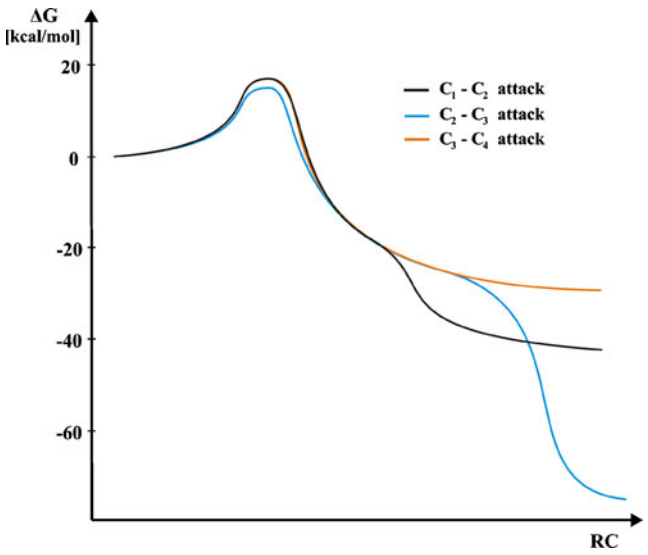

Fig. 5 Energetics of reactions of permanganate with phenolate

The results of calculations of Gibbs free energies of activation and reactions are given in Table 1. In the gas phase the reaction with ozone exhibits the lowest activation Gibbs free energy of about 15 kcal mol^{-1}. Reactions with molecular oxygen and permanganate are characterized by moderate activation free energies in the range of 25–30 kcal mol^{-1}. The reaction with perchlorate exhibits the highest activation free energy. The reaction with permanganate is considerably more exothermal than the other ones although it is much less exothermic than the corresponding reaction with trichloroethene [41].

Energetics in the liquid phase are quite similar with barriers being lower and exothermicity being larger. The sole exception is the activation barrier of the reaction between benzene and dioxygen. In this case the activation barrier increases substantially, by 17 kcal mol^{-1} in the liquid phase. This different trend is connected with a substantially different transition state structure for these reactions in comparison with the remaining three; the bond between C1 and O1 atoms is practically formed in the transition state while the C2-O2 distance decreases significantly, by about 0.17 Å (see Table 2) in going from the gas phase to the liquid phase. In the case of reactions with permanganate and ozone both these bonds elongate on the transfer to the liquid phase, while in the case of perchlorate one bond is considerably elongated (by about 0.25 Å) while the other shortens only slightly (0.04 Å).

Table 2 details bond distances and valence angles around the reactive centers. Data is given for transition states (TS) as well as for complexes of reactants (R) and for the products (P) obtained from the IRC procedure. Differences between geometries of the corresponding transition states are best illustrated by Fig. 2. In reactions with permanganate and ozone two C-O bonds are formed synchronically while in the case of perchlorate only one oxygen atom approaches the C-C bond of the benzene ring. As discussed above, with dioxygen two C-O bonds are formed but in a much unsynchronized manner.

Our main objective is to predict CSIA carbon isotopic fractionation (ε_{CSIA}) associated with the studied reactions. Since natural abundance of ^{13}C isotope is very low (about 1.1 %) the probability of finding multi-labeled molecules is

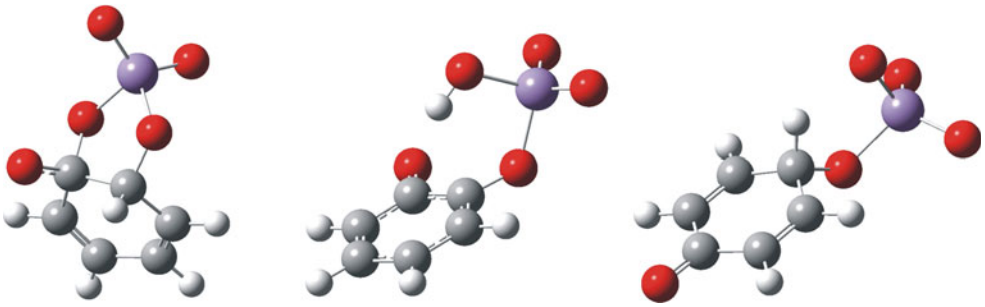

Fig. 6 Products of reaction between permanganate and deprotonated form of phenol, from left attack at: C_1-C_2, C_2-C_3, C_3-C_4

very low and can be neglected. Thus the CSIA carbon isotopic fractionation factor corresponds to the average value of individual isotope fractionation factors of carbon atoms at all positions. We have calculated CSIA carbon isotopic fractionations from individual kinetic isotope effects (KIEs) of individual carbon atoms in the aromatic ring of benzene, using our ISOEFF program, which can be converted into fractionation factors by using Eq. 1. Values of individual isotope effects and the resulting CSIA carbon isotopic fractionation for oxidation of benzene are collected in Table 3. The relative values of ε_{CSIA} parallel trends observed for activation barriers; except for the reaction with dioxygen they are smaller in the aqueous solution. From the isotopic forensic point of view (i.e., identification of the origin of a compound [46]) only the reaction with perchlorate in the liquid phase can be easily distinguished on the basis of ε_{CSIA} since it is about 3 ‰ different from values obtained for the other reactions.

Phenol

The reaction pattern to be considered becomes more complicated when substituents of the benzene ring are present. This is illustrated in Figs. 3 and 4 on the example of reaction of phenol with permanganate. The attack of the oxidant on different C-C bonds of the ring is not equivalent any more. In the following discussion we consider only aqueous solution. Phenol has been chosen as an example because it introduces yet another complication; it may be protonated or deprotonated depending on the pH of the solution.

Values of the Gibbs free energies of activation collected in Table 4 lead to a few interesting conclusions. First, deprotonated forms react much more easily with permanganate than the protonated ones, the difference is about 10 kcal mol^{-1}. However, the products of the substitution at C_1-C_2 and C_3-C_4 of the phenolate are relatively less stable than their protonated counterparts. The lower exothermicity of the latter reaction comes from significant dearomatization of the benzene ring. The high stability of the product of the reaction at the C_2-C_3 bond on the other hand results from the proton transfer that causes rearomatization of the phenolate ring. This is illustrated in Figs. 5 and 6 that show IRC paths for reactions of phenolate with permanganate and structures of products, respectively. Secondly, the reaction characterized by the lowest activation barrier is different for protonated (attack at C_3-C_4) and deprotonated (attack at C_2-C_3) forms. Finally, compared to unsubstituted reactant (benzene) even the reaction with the lowest activation barrier (22.9 kcal mol^{-1}) is by 1.7 kcal mol^{-1} more energetically demanding, suggesting that substituents (at least those similar to hydroxyl group) cause an aromatic pollutant to be harder to oxidize than benzene.

Table 5 Calculated carbon kinetic isotope effects and fractionation factors on protonated and deprotonated form of phenol reactions with permanganate

Position	Protonated form			Deprotonated form		
	C_1-C_2	C_2-C_3	C_3-C_4	C_1-C_2	C_2-C_3	C_3-C_4
C_1	1.0213	1.0002	1.0010	1.0026	0.9998	1.0006
C_2	1.0196	1.0184	1.0004	1.0242	1.0226	1.0010
C_3	1.0007	1.0199	1.0198	1.0027	1.0018	1.0013
C_4	0.9996	1.0004	1.0217	1.0003	1.0011	1.0213
C_5	1.0014	0.9984	1.0007	1.0022	0.9994	1.0019
C_6	1.0012	1.0017	0.9989	0.9996	1.0012	0.9996
ε_{CSIA} [‰]	−7.24	−6.56	−7.13	−5.22	−4.31	−4.19

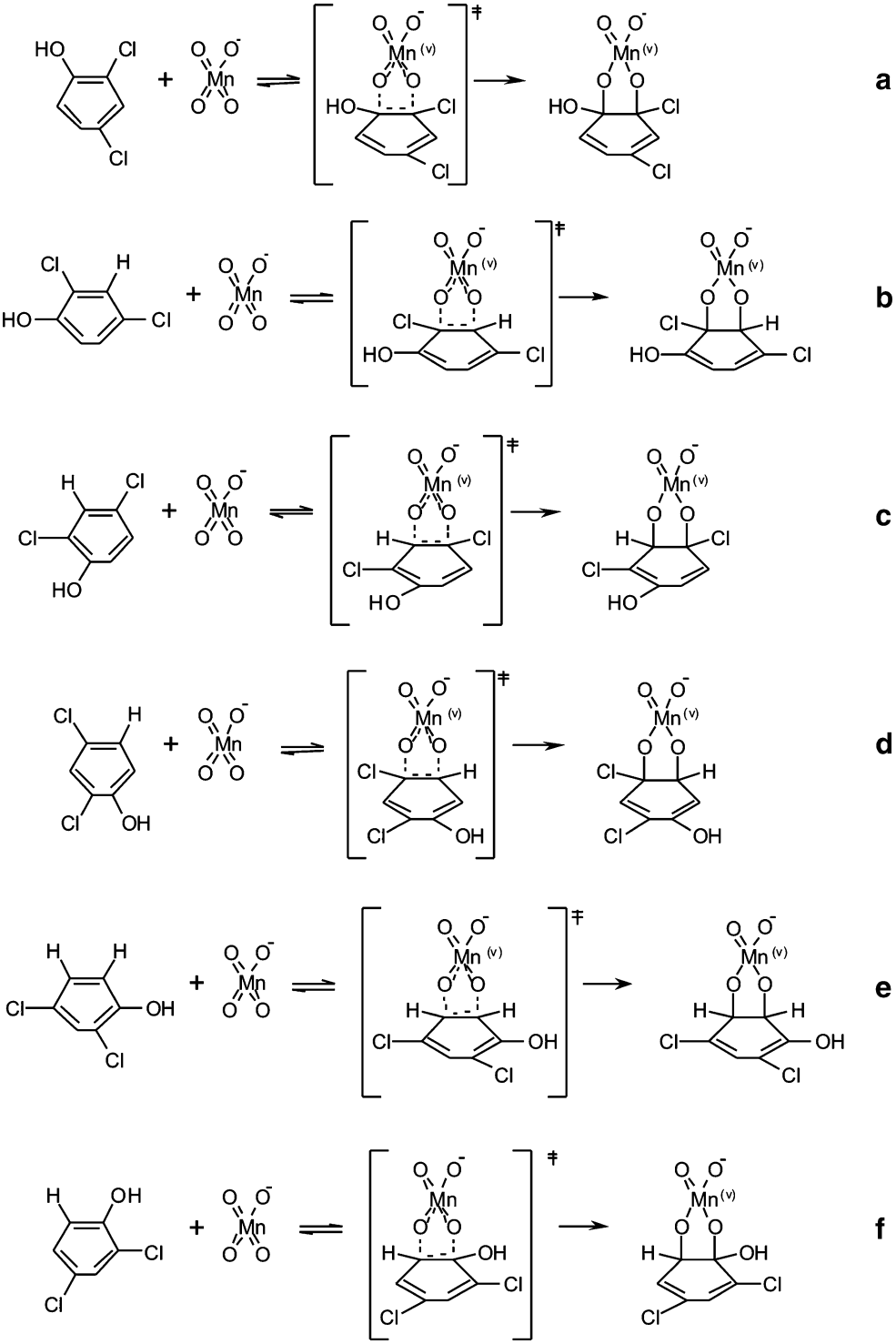

Fig. 7 Modeled reactions of MnO_4^- and protonated form of 2,4-dichlorophenol; attack at the position (**a**) C_1-C_2, (**b**) C_2-C_3, (**c**) C_3-C_4, (**d**) C_4-C_5, (**e**) C_5-C_6, (**f**) C_1-C_6

It should be noticed that only in the case of the attack at the C_1-C_2 bond two permanganate oxygen atoms make bonds to the aromatic ring. The formation of a C-O-Mn-O-C ring is, however, stepwise – first the oxygen atom of permanganate attacks the *ortho* position of the ring, then the molecule rotates (dihedral angle $\Phi_{C1\text{-}C2\text{-}O\text{-}O}$ changes from −36.3° to -23.6°) and subsequently the second oxygen atom attacks the C_1 carbon of the aromatic ring. In the case of the reaction at the C_3-C_4 bond of phenolate, two oxygen atoms of permanganate are located over the C_4-H bond and the attack on the ring occurs at the *para* position, resulting in the H-C_4-O_1-Mn-O_2 ring formation

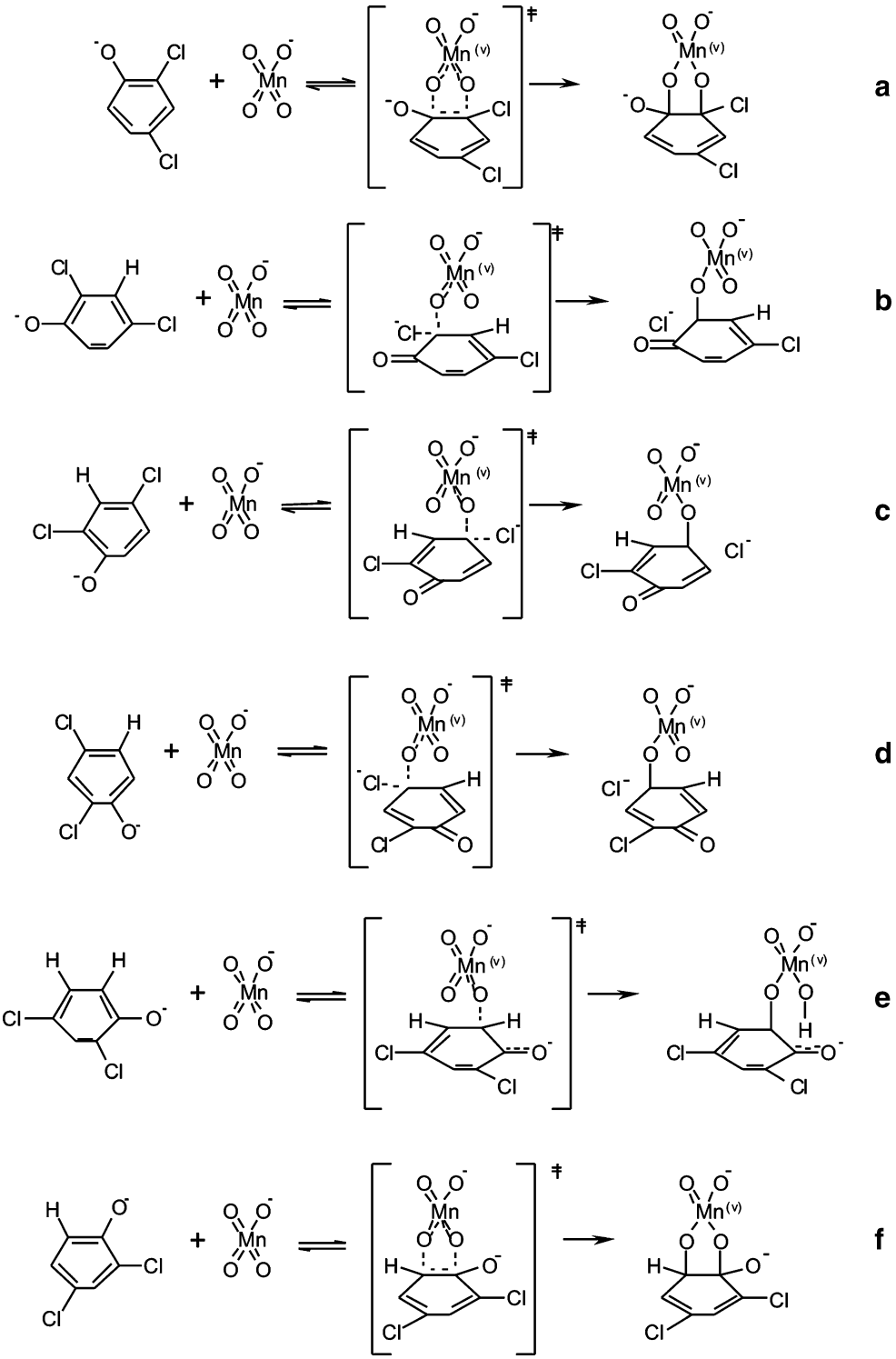

Fig. 8 Modeled reactions of MnO_4^- and deprotonated form of 2,4-dichlorophenol, attack at the position (**a**) C_1-C_2, (**b**) C_2-C_3, (**c**) C_3-C_4, (**d**) C_4-C_5, (**e**) C_5-C_6, (**f**) C_1-C_6

that is perpendicular to the aromatic ring. In this case the ring is not relaxed and the two Mn-O bonds are elongated; Mn-O_1 is extended to 1.84 Å while Mn-O_2 is extended to 1.72 Å. In the case of the reaction at the C_2-C_3 bond, permanganate is situated over the ring in the way similar to the reaction of the protonated form. The imaginary frequency includes vibrations of both oxygen atoms of permanganate although not symmetrically. In the final structure only one oxygen atom is attached to the carbon (in *ortho* position). Furthermore, the permanganate moiety is twisted and the proton is transferred from the ring to the oxygen atom similarly to the product of the reaction at the

C_3-C_4 bond discussed above. Analogically to the attack at the C_3-C_4 bond also in this reaction formation of the product is not associated with the relaxation of the aromatic ring.

As illustrated by data collected in Table 5, KIEs of individual carbon atoms of phenol lead to CSIA isotopic fractionation factors that are smaller than the one obtained for benzene in the aqueous solution (−7.62 ‰) and even smaller by 2 – 3 ‰ when the reaction proceeds via the deprotonated form. This is the result of differences in the attack modes; significant isotope effects are observed for two carbon positions when the protonated form reacts while only one position exhibits significant isotope effect in the case of phenolate.

2,4-dichlorophenol

In order to further evaluate the influence of substituents we have considered dichloroderivatives of phenol. These new substituents complicate the situation even further since any attack at the C-C bond of the ring is now unique thus reactions at all six bonds C_1-C_2, C_2-C_3, C_3-C_4, C_4-C_5, C_5-C_6, C_1-C_6 need to be considered explicitly. These reactions are shown schematically in Fig. 7 for the protonated form and in Fig. 8 for the enolate form while the energetic data is collected in Table 6.

Despite the loss of symmetry the results obtained for 2,4-dichlorophenol are quite similar to those obtained for the unsubstituted phenol although a few subtle differences can be noticed. In the case of the protonated form attacks at bonds C_3-C_4, C_4-C_5, and C_1-C_6 are energetically favored with the first one having the lowest activation barrier. Exothermicity of all six reactions is also at the same level with the exception of the attack at the C_5-C_6 bond in which products are destabilized by about 10 kcal mol^{-1}. The situation is slightly different for the deprotonated form.

Table 6 Activation Gibbs free energies and exothermicity of investigated reactions of protonated and deprotonated form of 2,4-dichlorophenol with permanganate ion

Position	Protonated form		Deprotonated form	
	$\Delta G^{\neq}$ [kcal/mol]	ΔG_R [kcal/mol]	$\Delta G^{\neq}$ [kcal/mol]	ΔG_R [kcal/mol]
C_1-C_2	27.5	−58.4	17.9	−49.1
C_2-C_3	24.6	−57.1	16.6	−36.4
C_3-C_4	22.4	−59.3	18.7	−36.6
C_4-C_5	23.1	−57.2	18.8	−37.4
C_5-C_6	25.0	−49.2	16.4	−77.2
C_1-C_6	23.4	−53.7	16.2	−41.3

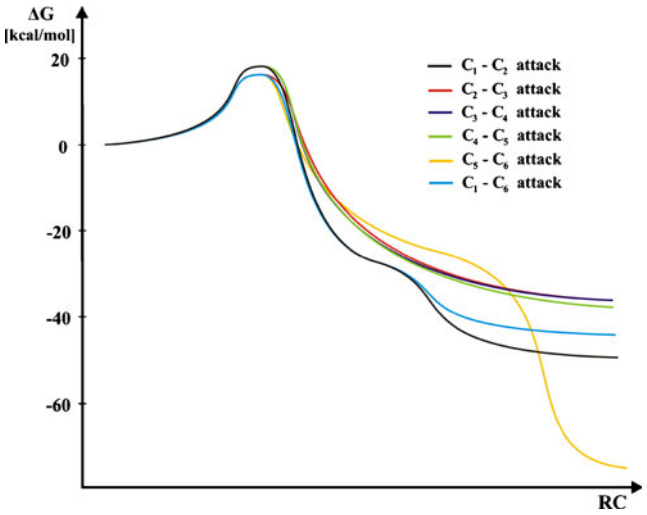

Fig. 9 Energy diagram of IRC calculations of modeled reactions of permanganate ion and deprotonated form of 2,4-dichlorophenol

Again activation barriers for the reactions of the deprotonated form are lower by a few kcal mol^{-1} than for the analogous reactions of the protonated form, with the attack at the C_1-C_6 bond being the most feasible. Product exothermicity is inversed; the most stable is the one formed by the attack at the C_5-C_6 bond. As illustrated in Fig. 9 this stabilization is due to the subsequent, barrier-less proton transfer to the oxygen atom of the permanganate moiety. In three cases however, (C_2-C_3, C_3-C_4, and C_4-C_5) the C-Cl bond is also broken in the products and the chloride anion is formed.

In Table 7 KIEs of individual carbon atoms of the aromatic ring of protonated and deprotonated forms of 2,4-dichlorophenol as well as the corresponding CSIA carbon isotopic fractionation factors are collected. As can be seen the variation in ε_{CSIA} is small among reactions occurring at different C-C bonds for both forms of 2,4-dichlorophenol. These values are on average slightly higher than those calculated for phenol and benzene, although the value obtained for the energetically most favorable pathway (attack at the C_3-C_4 bond) is practically the same as the value obtained for benzene. The difference between ε_{CSIA} for protonated and unprotonated is very similar to that calculated for phenol.

Conclusions

Our studies have shown that benzene oxidation by permanganate proceeds with an activation barrier equal to 21.2 kcal mol^{-1} (which is significantly higher than in the case TCE for which the barrier is 9.4 kcal mol^{-1}). The exothermicity of the aromatic ring oxidation is about

45.6 kcal mol^{-1} which is lower than in the case of chlorinated acyclic compounds. Benzene oxidation by permanganate leads to a cyclic product which is almost symmetrical. Oxidation mechanisms by permanganate and ozone are quite similar – both reactions proceed at two aromatic carbon atoms and with the formation of a cyclic product. In the case of these two oxidants, the change from the gas to liquid phase has little effect on the energetics of the reaction and on the isotopic fractionation factors. The situation is different for oxidation with perchlorate and dioxygen. The carbon isotopic fractionation factor for the oxidation of benzene by perchlorate changes by about 2 ‰ from the gas phase to aqueous solution although the involvement of two carbon atoms in the formation of the three-member C-O-C ring in the aqueous solution is almost identical. This increase in the symmetry of the C-O-C ring in the liquid phase (compared to the gas phase) results in the reduction of the activation barrier by 10 kcal mol^{-1}. The reaction of benzene with dioxygen shows the biggest change of the activation barrier; it increases by almost 20 kcal mol^{-1} for aqueous solution compared to the gas phase. The corresponding difference in isotopic fractionation factor is over 1 ‰ and results from the increased value of KIE of the aromatic carbon atom involved in the reaction.

In the case of phenol and its derivatives several pathways are possible. Our results agree with experimental data; oxidation of phenol leads to muconic acid through *o*- or *p*-benzoquinone [24] while oxidation of 2,4-dichlorophenol leads mainly to dichloromuconic acid via 2,4-dichlorocatechol [47]. Furthermore, we have found that the activation barrier of the deprotonated form of phenol and its chlorinated derivatives is about 10 kcal mol^{-1} lower than those for reactions of corresponding protonated forms. This behavior has also been observed experimentally [48–50]. Taking into account that protonated and deprotonated forms of phenols are both present under aqueous conditions we can conclude that permanganate reacts preferentially with the deprotonated. It also means that increasing the basicity of a solution (and in the consequence increasing the concentration of the deprotonation form of phenols) have positive impact on permanganate degradation of phenols and its chloroderivatives. It should also be noted that activation barriers of permanganate oxidation of protonated forms of phenolic compounds studied here are even slightly higher than in the case of benzene. Together with the fact that ISCO methodology targets better phenols than benzene [15] this also points to the role of deprotonation in the oxidative degradation of phenols. Values of carbon isotopic fractionation factors associated with reactions of the protonated form of phenol and its chloroderivatives are higher than those for the deprotonated species. This is due to the fact that in the case of the protonated forms reactions proceed at two aromatic carbon atoms while in the case of deprotonated forms only at one aromatic carbon atom. These values are also higher for dichloroderivatives than for phenol. Obtained differences between values of fractionation factors of the corresponding protonated and deprotonated forms of the investigated phenols and their chloroderivatives are quite small but should be sufficient to distinguish different mechanisms of degradation using CSIA methodology.

Table 7 Calculated carbon kinetic isotope effects and fractionation factors on protonated and deprotonated form of 2,4-dichlorophenol reactions with permanganate

Position	Protonated form					
	C_1-C_2	C_2-C_3	C_3-C_4	C_4-C_5	C_5-C_6	C_1-C_6
C_1	1.0260	1.0004	1.0002	1.0021	0.9999	1.0230
C_2	1.0224	1.0201	0.9991	1.0031	1.0028	0.9995
C_3	1.0010	1.0214	1.0219	1.0013	1.0019	1.0018
C_4	1.0002	1.0013	1.0203	1.0223	1.0010	1.0021
C_5	1.0016	1.0011	1.0013	1.0219	1.0216	1.0006
C_6	0.9997	1.0015	1.0017	1.0009	1.0183	1.0195
ε_{CSIA} [‰]	−8.39	−7.59	−7.38	−8.55	−7.55	−7.71
	Deprotonated form					
C_1	1.0017	1.0002	0.9998	0.9994	1.0001	1.0034
C_2	1.0291	1.0259	1.0007	1.0003	1.0011	1.0005
C_3	1.0013	1.0010	1.0041	1.0003	1.0017	1.0021
C_4	0.9999	1.0023	1.0268	1.0282	1.0022	1.0011
C_5	1.0022	1.0022	1.0004	1.0049	1.0033	1.0021
C_6	1.0011	1.0014	0.9993	1.0010	1.0251	1.0245
ε_{CSIA} [‰]	−5.80	−5.95	−5.12	−5.65	−5.55	−5.57

Acknowledgments The research leading to these results has received funding from the European Community's Seventh Framework Programme (FP7/2009-20012) under grant agreement no 212781 and accompanying grant 1130/7.PRUE/2009/7 from the Ministry of Higher Education and Science, Poland. Computing time allocation at Cyfronet, Krakow is acknowledged.

References

1. WHO(IARC), International Agency for Research on Cancer (IARC) (1987) IARC Monographs on the Evaluation of Carcinogenic Risk to Humans. IARC, Lyon, Suppl. 7
2. U.S. EPA. (1998) Carcinogenic Effects of Benzene: An Update, EPA/600/P-97/001-F, U.S. Environmental Protection Agency, Washington, DC
3. Budavari S (1996) The Merck Index: An Encyclopedia of Chemical, Drugs, and Biologicals. Merck, Whitehouse Station, NJ
4. Warner MA, Harper JV (1985) Cardiac dysrhythmias associated with chemical peeling with phenol. Anesthesiology 62:366–367
5. ATSDR (Agency for Toxic Substances and Disease Registry) (2007) CERCLA Priority List of Hazardous Substances, U.S. Department of Health and Human Services, Agency for Toxic Substances and Disease Registry, Division of Toxicology and Environmental Medicine, Atlanta, GA, in cooperation with U. S. Environmental Protection Agency, http://www.atsdr.cdc.gov/cercla/07list.html (accessed 09.09.2010)
6. ATSDR (Agency for Toxic Substances and Disease Registry) (2005) Toxicological Profile for Benzene. Agency for Toxic Substances and Disease Registry, US Public Health Service
7. Gad SN, Saad SA (2008) Effect of environmental pollution by phenol on some physiological parameters of *Oreochromis niloticus*. Global Vet 2:312–319
8. Fleeger JW, Carman KR, Nisbet RM (2003) Indirect effect of contaminants in aquatic ecosystem. Sci Total Environ 3170:207–233
9. Mukherjee D, Bhttacharya S, Kumar V, Moitra J (1990) Biological significance of. Phenol accumulation in different organs of a murrel, *Chamnna punctatus* and the common carp *Cyprinus carpio*. Biomed Environ Sci 3:337–342
10. ATSDR (Agency for Toxic Substances and Disease Registry) (1989) Toxicological Profile for Phenol. Agency for Toxic Substances and Disease Registry, US Public Health Service
11. Pera-Titus M, Garcia-Molina V, Banos MA, Gimenez J, Esplugas S (2004) Degradation of chlorophenols by means of advanced oxidation processes: a general review. Appl Catal B 47:219–256
12. Laoufti NA, Tassalit D, Bentahar F (2008) The degradation of phenol in water solution by TiO_2 photocatalisys in helical reactor. Global NEST J 10:404–418
13. Huang K, Zhao Z, Hoag G, Dahmani A, Block P (2005) Degradation of volatile organic compounds with thermally activated persulfate oxidation. Chemosphere 61:551–560
14. Liang CJ, Bruell CJ, Marley MC, Sperry KL (2004) Persulfate oxidation for in situ remediation of TCE. I. Activated by ferrous ion with and without a persulfate-thiosulfate redox couple. Chemosphere 55:1213–1223
15. Nadim F, Huang K, Dahmani A (2006) Remediation of soil and ground water contaminated with PAH using heat and Fe(II)-EDTA catalyzed persulfate oxidation. Water Air Soil Pollut Focus 6:227–232
16. Zazo JA, Casas JA, Mohedano AF, Gilarranz MA, Rodriguez JJ (2005) Chemical Pathway and Kinetics of Phenol Oxidation by Fenton's Reagent. Environ Sci Technol 39:9295–9302
17. Munter R (2001) Advanced oxidation processes. Current status and prospects. Proc Est Acad Sci Chem 50:59–80
18. Freeman F (1975) Possible criteria for distinguishing between cyclic and acyclic activated complexes and among cyclic activated complexes in addition reactions. Chem Rev 75:439–490
19. Gardner KA, Mayer JM (1995) Understanding C-H bond oxidations: H* and H- transfer in the oxidation of toluene by permanganate. Science 269:1849–1851
20. Rudakov ES, Lobachev VL (1994) The kinetics, kinetic isotope effects, and substrate selectivity of alkylbenzene oxidation in aqueous permanganate solutions. II. Reaction with HMnO4. Kinet Catal 35:180–187
21. Rudakov ES, Lobachev VL (2000) The first step of oxidation of alkylbenzenes by permanganates in acidic aqueous solutions. Russ Chem Bull 49:761–777
22. Mvula E, Naumov S, von Sonntag C (2009) Ozonolysis of Lignin Models in Aqueous Solution: Anisole, 1,2-Dimethoxybenzene, 1,4-Dimethoxybenzene, and 1,3,5-Trimethoxybenzene. Environ Sci Technol 43:6275–6282
23. Koester CJ, Simonich SL, Esser BK (2003) Environmental Analysis. Anal Chem 75:2813–2829
24. Elsner M, Zwank L, Hunkeler D, Schwarzenbach RP (2005) A new concept linking observable stable isotope fractionation to transformation pathways of organic pollutants. Environ Sci Technol 39:6896–6916
25. Dybala-Defratyka A, Szatkowski L, Kaminski R, Wujec M, Siwek A, Paneth P (2008) Kinetic isotope effects on dehalogenations at an aromatic carbon. Environ Sci Technol 42:7744–7750
26. U.S. EPA (2008) A Guide for assessing biodegradation and source indentification of organic groundwater contaminants usung Compound Specific Isotope Analysis (CSIA). EPA/600/R-08/148, U.S. Environmental Protection Agency, Washington, DC
27. Frisch MJ et al. (2004) Gaussian 03, Revision E.01. Gaussian Inc, Wallingford
28. Frisch MJ et al. (2009) Gaussian 09, Revision A.02. Gaussian Inc, Wallingford, CT
29. Zhao Y, Schultz NE, Truhlar DG (2006) Design of density functionals by combining the method of constraint satisfaction with parametrization for thermochemistry, thermochemical kinetics, and noncovalent interactions. J Chem Theory Comput 2:364–382
30. Zhao Y, Truhlar DG (2008) Density functionals with broad applicability in chemistry. Acc Chem Res 41:157–167
31. Hariharan PC, Pople JA (1973) Influence of polarization functions on MO hydrogenation energies. Theor Chim Acta 28:213–222
32. Ditchfield R, Hehre WJ, Pople JA (1971) Self-consistent molecular-orbital methods. IX. Extended Gaussian-type basis for molecular-orbital studies of organic molecules. J Chem Phys 54:724–728
33. Francl MM, Pietro WJ, Hehre WJ, Binkley JS, Gordon MS, DeFrees DJ, Pople JA (1982) Self-consistent molecular orbital methods. XXIII. A polarization-type basis set for second-row elements. J Chem Phys 77:3654–3665
34. Clark T, Chandrasekhar J, Spitznagel GW, Von Ragué SP (1983) Efficient diffuse function-augmented basis sets for anion calculations. III. The 3-21+G basis set for first-row elements, lithium to fluorine. J Comput Chem 4:294–301
35. Frisch MJ, Pople JA, Binkley JS (1984) Self-consistent molecular orbital methods. XXV. Supplementary functions for Gaussian basis sets. J Chem Phys 80:3265–3269
36. Miertus S, Scrocco E, Tomasi J (1981) Electrostatic interaction of a solute with a continuum. A direct utilization of ab initio molecular potentials for the prevision of solvent effects. Chem Phys 55:117–129
37. Rappe AK, Casewit CJ, Colwell KS, Goddard WA III, Skiff WM (1992) UFF, a full periodic table force field for molecular mechanics and molecular dynamics simulations. J Am Chem Soc 114:10024–10035

38. Dybala-Defratyka A, Adamczyk P, Paneth P (2011) A DFT study of Trichloroethene reaction with permanganate in aqueous solution. Env Sci Technol 45(7):3006–3011
39. McWeeny R, Dierksen G (1968) Self-consistent perturbation theory. II. Extension to open shells. J Chem Phys 49:4852–4856
40. Peng C, Ayala PY, Schlegel HB, Frisch MJ (1996) Using redundant internal coordinates to optimize equilibrium geometries and transition states. J Comput Chem 17:49–56
41. Reed AE, Weinhold F (1983) Natural bond orbital analysis of near-Hartree–Fock water dimer. J Chem Phys 78:4066–4073
42. Fukui K (1970) Formulation of the reaction coordinate. J Phys Chem 74:4161–4163
43. Anisimov V, Paneth P (1999) ISOEFF98. A program for studies of isotope effects using Hessian modifications. J Math Chem 26:75–86
44. Bigeleisen J (1949) The relative reaction velocities of isotopic molecules. J Chem Phys 17:675–678
45. Hofstetter TB, Schwarzenbach RP, Bernasconi SM (2008) Assessing transformation processes of organic compounds using stable isotope fractionation. Environ Sci Technol 42:7737–7743
46. Fox AD, Hobson KA, Ekins G, Grantham M, Green AJ (2010) Isotopic forensic analysis does not support vagrancy for a Marbled Duck shot in Essex. Br Birds 103:464–467
47. Mueller R, Lingens F (1986) Microbial degradation of halogenated hydrocarbons: a biological solution to pollution problems. Angew Chem Int Ed Engl 25:779–789
48. Tratnyek PG, Hoigne J (1994) Kinetics of reactions of chlorine dioxide (OClO) in water. II. Quantitative structure-activity relationships for phenolic compounds. Water Res 28:57–66
49. Tratnyek PG, Hoigne J (1991) Oxidation of substituted phenols in the environment: a QSAR analysis of rate constants for reaction with singlet oxygen. Environ Sci Technol 25:1596–1604
50. Tratnyek PG (1998) Correlation analysis of the environmental reactivity of organic substances. In: Macalady DL (ed) Perspectives in Environmental Chemistry. Oxford, New York, pp 167–194